

# **GenoWAP: Post-GWAS Prioritization Through Integrated Analysis of Genomic Functional Annotation**

Qiongshi Lu<sup>1</sup>, Xinwei Yao<sup>2</sup>, Yiming Hu<sup>1</sup>, Hongyu Zhao<sup>1,3,4\*</sup>

<sup>1</sup> Department of Biostatistics, Yale School of Public Health, New Haven, CT, USA

<sup>2</sup> Yale College, New Haven, CT, USA

<sup>3</sup> Program of Computational Biology and Bioinformatics, Yale University, New Haven, CT, USA

<sup>4</sup> VA Cooperative Studies Program Coordinating Center, West Haven, CT, USA

\* To whom correspondence should be addressed:

Dr. Hongyu Zhao  
Department of Biostatistics  
Yale School of Public Health  
60 College Street,  
New Haven, CT, 06511, USA  
[hongyu.zhao@yale.edu](mailto:hongyu.zhao@yale.edu)

## **Running Head**

Post-GWAS Prioritization

## **Abstract**

### **Motivation**

Genome-wide association study (GWAS) has been a great success in the past decade. However, significant challenges still remain in both identifying new risk loci and interpreting results. Bonferroni-corrected significance level is known to be conservative, leading to insufficient statistical power when the effect size is moderate at risk locus. Complex structure of linkage disequilibrium also makes it challenging to separate causal variants from nonfunctional ones in large haplotype blocks.

### **Results**

We describe GenoWAP, a post-GWAS prioritization method that integrates genomic functional annotation and GWAS test statistics. The effectiveness of GenoWAP is demonstrated through its applications to Crohn's disease and schizophrenia using the largest studies available, where highly ranked loci show substantially stronger signals in the whole dataset after prioritization based on a subset of samples. At the single nucleotide polymorphism (SNP) level, top ranked SNPs after prioritization have both higher replication rates and consistently stronger enrichment of eQTLs. Within each risk locus, GenoWAP is also able to distinguish functional sites from groups of correlated SNPs.

### **Availability and Implementation**

GenoWAP is freely available on the web at <http://genocanyon.med.yale.edu/GenoWAP>

## Introduction

In the past ten years, genome-wide association studies (GWAS) have been designed and applied to identify disease genes for almost all complex diseases. As of January 15, 2015, 15,216 single nucleotide polymorphisms (SNP) from over 2,000 publications have been documented in the GWAS Catalog (Hindorff, et al., 2009). Despite its great success in identifying disease-associated loci, scientists have noted several limitations of current GWAS approaches. First, although linkage disequilibrium (LD) is the basis of GWAS, it also hinders the interpretation of association results. Due to the complex LD structure among SNPs, it is the disease-associated haplotype blocks containing hundreds of thousands of nucleotides that are identified in GWASs. Therefore, the resolution of GWAS is not sufficient for distinguishing causal variants from a large group of correlated SNPs, especially in non-coding regions where the mechanism of genomic function is still largely unknown (Cooper and Shendure, 2011; Visscher, et al., 2012; Ward and Kellis, 2012). Second, although Bonferroni-corrected significance threshold (e.g.  $5 \times 10^{-8}$ ) is widely accepted as the standard cutoff in GWAS analysis, it is well known that Bonferroni correction is too conservative when the number of hypotheses is large and there are many weak to moderate signals. In fact, for most complex diseases, numerous genomic loci are involved in disease etiology while each locus only has a moderate effect size. Therefore, studies based on high-throughput genomic scan may be underpowered if the sample size is not large enough. This has led to so-called missing heritability, which refers to the gap between the narrow-sense heritability estimated from twin/pedigree analysis and the proportion of the variance explained by significant SNPs identified from GWAS, that has been reported for many diseases (Manolio, et al., 2009; Witte, et al.,

2014). One explanation of missing heritability is the insufficient statistical power to identify all the disease-associated SNPs (Eichler, et al., 2010).

Variant prioritization techniques are crucial for post-GWAS analysis on different scales. Locally, it can reveal truly functional variants within each significant locus. Globally, signals at some loci can be enhanced if proper prior information is used. Many variant prioritization methods have been proposed (Hou and Zhao, 2013). Supervised-learning-based statistical tools for predicting deleterious variants are probably the richest among available approaches. So far, most of the existing deleteriousness prediction tools only focus on protein-coding genes in the human genome. However, coding-region-based tools are not sufficient for post-GWAS prioritization because nearly 90% of the significant SNPs identified in GWAS reside in the non-coding genome (Hindorff, et al., 2009). A few tools targeting non-coding variants have been proposed (Fu, et al., 2014; Kircher, et al., 2014; Ritchie, et al., 2014; Shihab, et al., 2015). Detailed comparisons of these methods were reviewed elsewhere (Cooper and Shendure, 2011; Wang, et al., 2015). Unlike the extensively studied protein-altering variants, very few non-coding pathogenic variants have been revealed so far (Ward and Kellis, 2012). Therefore, existing non-coding variant prioritization tools based on supervised-learning may suffer from the potentially biased training data. Their performance in post-GWAS prioritization remains to be further investigated. Finally, although deleteriousness of a single SNP is crucial for identifying causal variants, it does not provide all the information needed in post-GWAS prioritization, where each SNP in GWAS also carries information of nearby variants that are not genotyped. A better informed post-GWAS prioritization method



should be able to measure the functional potential for the surrounding region of each genotyped marker.

Recently, Lu et al. developed GenoCanyon, a statistical framework to predict functional non-coding regions in the human genome through integrated analysis of multiple biochemical signals and genomic conservation measures (Lu, et al., 2015). Its unsupervised-learning framework makes GenoCanyon suffer less from our limited knowledge of non-coding genome. Moreover, since the resolution of its functional prediction is at the nucleotide level, it is possible to use GenoCanyon scores to evaluate the surrounding region of each genotyped SNP. In this paper, we propose GenoWAP (Genome Wide Association Prioritizer), a post-GWAS prioritization method that integrates GenoCanyon functional prediction and GWAS p-values. We apply the method on two smaller GWASs of Crohn's disease and schizophrenia, respectively, to prioritize SNPs. The performance is evaluated using the results from large GWAS meta-analyses of these two diseases. Compared to the top loci ranked on p-values only, top ranked loci after prioritization tend to show substantially stronger signals in large GWAS studies. Within each locus, GenoWAP is able to distinguish true signals among highly correlated SNPs. The method has the potential to reduce noises caused by LD and rescue marginal signals in GWASs with insufficient sample sizes.

## **Methods**

### **Statistical model**

For each SNP, we define  $Z$  to be the indicator of general functionality, and define  $Z_D$  to be the indicator of disease-specific functionality. More specifically, if a SNP or its surrounding region is active in any genomic functional pathway, then  $Z$  equals to 1. If this SNP or the surrounding region is involved in the disease pathway, then  $Z_D$  equals to 1. For each SNP, we use  $p$  to denote its p-value obtained from the standard GWAS analysis.

The goal of post-GWAS prioritization is to assign each SNP a new score that measures its importance. A reasonable quantity is the conditional probability of being disease-specific functional given the p-value, i.e.  $P(Z_D = 1|p)$ . Using Bayes formula, we can rewrite the conditional probability as below:

$$P(Z_D = 1|p) = \frac{f(p|Z_D = 1) \times P(Z_D = 1)}{f(p|Z_D = 1) \times P(Z_D = 1) + f(p|Z_D = 0) \times P(Z_D = 0)} \quad (1)$$

Based on the definitions of  $Z$  and  $Z_D$ , we know that the SNPs satisfying  $Z_D = 1$  must be a subset of the SNPs satisfying  $Z = 1$ . This is because if a SNP is disease-specific functional, then it has to be functional in the general sense. Therefore, we get the following formula.

$$\begin{aligned} P(Z_D = 1) &= P(Z = 1, Z_D = 1) \\ &= P(Z_D = 1|Z = 1) \times P(Z = 1) \end{aligned} \quad (2)$$

Therefore, in order to calculate the conditional probability  $P(Z_D = 1|p)$  for a marker, we need its prior probability of being functional, i.e.  $P(Z = 1)$ ; we also need the p-value density for disease-specific functional markers, i.e.  $f(p|Z_D = 1)$ , and the p-value density for markers that are not related to the disease, i.e.  $f(p|Z_D = 0)$ ; finally, we need an estimate for the conditional probability of being disease-specific functional given the marker is functional in the general sense, i.e.  $P(Z_D = 1|Z = 1)$ .

## Estimation

Recently, Lu et al. developed GenoCanyon, an unsupervised-learning-based statistical framework that predicts the functional potential for each nucleotide in the human genome (Lu, et al., 2015). For each SNP in our dataset, we use the mean GenoCanyon functional score of its surrounding 10,000 base pairs as the prior probability  $P(Z = 1)$ . Different from using variant-based annotation tools as the prior knowledge, this prior information not only measures the importance of the genotyped marker, but also evaluates its surrounding region where the ungenotyped causal variants may reside.

Next, we partition all the SNPs into functional ( $Z = 1$ ) and non-functional ( $Z = 0$ ) subgroups based on the calculated mean GenoCanyon score with cutoff 0.1. Since the GenoCanyon functional score has a bimodal pattern, this partition is not sensitive to the cutoff choice. There are two major reasons why we do the partition. First, this can be viewed as a noise reduction step. After removing the non-functional markers, the signal pattern in the functional subgroup is amplified (**Figure 1**). The proportion of disease-related markers in the remaining (functional) subgroup also increased, which leads to

more stable estimates in the following steps. Second, we can now empirically estimate the p-value density for non-functional markers, i.e.  $f(p|Z = 0)$ . Since the p-values are acquired from a disease-specific case-control study, we assume that the p-values for markers that are not related to the disease should behave just like the p-values for markers that are not functional entirely. Mathematically, this assumption is characterized as the equation below.

$$f(p|Z_D = 0) = f(p|Z = 0) \quad (3)$$

Based on this assumption, we can estimate  $f(p|Z_D = 0)$  using the p-values for SNPs in the non-functional subgroup. Notably, it may seem natural to assume  $(p|Z_D = 0)$  follows a uniform distribution. However, the p-value of a marker with  $Z_D = 0$  can actually be driven by a nearby disease-related marker due to LD. The empirically estimated density can capture a certain amount of LD information, which is complex and non-trivial to model. Moreover, it is common to see some variants with low minor allele frequencies in GWAS samples. The p-values for these markers will form a spike near 1 in the p-value density. The empirically estimated density is also able to account for this artifact. We propose to use histogram for density estimation, because it has stable performance near the boundary. In fact, the p-value boundary near 0 is where the real signals reside, and the boundary near 1 occasionally has the artifact issue caused by rare variants. Histogram is able to capture both issues. Moreover, the sample size in this framework is the number of markers, which is usually large in GWAS studies. Therefore histogram is a reasonable choice for density estimation. The number of bins is chosen based on cross-validation.

It still remains to estimate the p-value density for disease-related markers  $f(p|Z_D = 1)$ , and the conditional probability  $P(Z_D = 1|Z = 1)$ . Now, we partition the functional subgroup ( $Z = 1$ ) into finer subgroups. First, based on equation (3), it is straightforward to show that

$$f(p|Z = 1, Z_D = 0) = f(p|Z_D = 0) = f(p|Z = 0) \quad (4)$$

Therefore, the p-value density for functional markers is the following mixture.

$$\begin{aligned} f(p|Z = 1) &= P(Z_D = 1|Z = 1) \times f(p|Z = 1, Z_D = 1) + P(Z_D = 0|Z = 1) \times f(p|Z = 1, Z_D = 0) \\ &= P(Z_D = 1|Z = 1) \times f(p|Z_D = 1) + P(Z_D = 0|Z = 1) \times f(p|Z_D = 0) \end{aligned} \quad (5)$$

In formula (5),  $f(p|Z_D = 0)$  has already been estimated in previous steps. We further assume a parametric form of  $f(p|Z_D = 1)$ . In a recent work of Chung et al., they showed that beta distribution is a robust approximation of p-value distribution under some general assumptions of SNP effect size (Chung, et al., 2014). We adopt the same assumption.

$$(p|Z_D = 1) \sim \text{Beta}(\alpha, 1), \quad 0 < \alpha < 1 \quad (6)$$

The constraint  $0 < \alpha < 1$  guarantees that a smaller p-value is more likely to occur than a larger p-value. Then, we apply the EM algorithm on all the p-values in the functional subgroup. One advantage of beta distribution assumption is that each iteration in the EM algorithm has a closed-form expression. In this way, we acquire the estimates for both

$P(Z_D = 1|Z = 1)$  and  $P(p|Z_D = 1)$ . Then, all missing pieces in formula (1) have been estimated. We calculate the conditional probability  $P(Z_D = 1|p)$  for all the SNPs using these estimates. This quantity is referred to as the posterior score in this paper.

## Results

### Application to Crohn's disease

Several GWASs of different scales have been performed for Crohn's disease. The largest GWAS meta-analysis, which identified 71 disease-associated loci, is one of the most successful GWASs to date (Franke, et al., 2010). We applied GenoWAP on a smaller Crohn's disease GWAS conducted by the North American National Institute of Diabetes and Digestive and Kidney Diseases (NIDDK) IBD Genetics Consortium, and tested the results using the large meta-analysis done by the International Inflammatory Bowel Disease Genetics Consortium (IIBDGC). Cohort information is listed in **Supplementary Table 1**. Details of both studies have also been reported previously (Franke, et al., 2010; Rioux, et al., 2007). It is worth noting that the samples in these two studies overlap with each other. However, the goal for this paper is not to replicate the detected signals in an independent cohort. Instead, we seek to better prioritize signals using only a small sample size. In order to test the performance, the results from the largest study available are used as the gold standard.

For each SNP in the dataset, define  $p$  to be the GWAS p-value, and define  $Z_D$  to be the indicator of disease-specific functionality. The posterior probability of being disease-

specific functional, i.e.  $P(Z_D = 1|p)$ , is used to prioritize SNPs (See **Methods**). This score will be referred to as the posterior score in the following sections. Test statistics of the NIDDK study were downloaded from dbGap (**Supplementary Table 1**). Among the 298,391 SNPs, 70 were deleted due to unavailable hg19 genomic locations. We calculated the posterior scores for the remaining 298,321 SNPs (**Supplementary Figure 1**). Test statistics of the IIBDGC meta-analysis were downloaded from the IIBDGC website (<http://www.ibdgenetics.org>). The dataset contains 953,241 SNPs, including 262,621 SNPs overlapping with the NIDDK dataset.

A total of 71 loci passed genome-wide significance level in the validation stage of IIBDGC meta-analysis, including 32 previously reported risk loci and 39 newly confirmed risk loci (Franke, et al., 2010). We ranked the 298,321 SNPs in the NIDDK study based on their p-values and posterior scores, respectively. Then, within each locus among the 71 loci, we compared the rank of the lowest p-value to the rank of the largest posterior score. 56 out of 71 loci (79%) had an improved rank, 3 loci (4%) had an equal rank, while only 12 loci (17%) had a reduced rank (**Supplementary Table 2**). The probability of having an increased rank is significantly higher than that of having a decreased rank ( $p\text{-value} = 3.11 \times 10^{-8}$ , one-sided binomial test).

Next, we compared the top 20 loci with the smallest p-values to the top 20 loci with the largest posterior scores in the NIDDK study. The locus information and the lowest meta-analysis p-value at each locus are listed in **Table 1**. 14 out of 20 loci are shared between the two lists. Interestingly, the posterior-specific loci, i.e. the loci that show up only in the

list based on posterior score, showed substantially stronger signals in the IIBDGC meta-analysis compared to the p-value-specific loci (**Table1, Figure 2a**). For example, the risk locus on chromosome 10q22 was a genome-wide significant locus in the meta-analysis (rs1250550,  $P_{meta} = 2.00 \times 10^{-10}$ ). Although the same SNP, rs1250550, had the lowest p-value at this locus in the NIDDK dataset ( $P_{NIDDK} = 5.95 \times 10^{-5}$ ), the signal was not strong enough to make this locus surpass other loci such as the one on chromosome 2q24 (rs6733000,  $P_{NIDDK} = 2.01 \times 10^{-5}$ , **Table 1**). However, with posterior scores, locus 10q22 was ranked as the 17<sup>th</sup> top locus, while the highest posterior score at locus 2q24 was only 0.0142, which agrees with its weak signal in the meta-analysis result ( $P_{meta} = 0.019$ ). Overall, two posterior-specific loci were genome-wide significant in the meta-analysis, while the lowest  $P_{meta}$  among the six p-value-specific loci was only  $1.10 \times 10^{-4}$ . These results show that our method can effectively reduce noises likely due to LD and chance and enhance true signals at disease risk loci.

To see if SNPs with high posterior scores are more enriched of eQTLs, we downloaded the whole-blood eQTL data from GTEx (<http://www.gtexportal.org>). The top 1000 SNPs based on p-values are not statistically significantly enriched for eQTLs (p-value = 0.076; hypergeometric test; fold enrichment = 1.39), while the enrichment for the top 1000 SNPs based on posterior scores is highly significant (p-value =  $1.46 \times 10^{-4}$ ; fold enrichment = 2.17). The difference becomes even more drastic when using the top 2000 SNPs, with p-values 0.018 and  $6.19 \times 10^{-11}$  (fold enrichment 1.43 and 2.56), respectively. When the number of top SNPs increases, the posterior-based approach



dominates the p-value-based approach in both enrichment p-value and fold change (**Figures 2b** and **2c**).

In order to show how our method performs locally, we chose two genome-wide significant loci from the IIBDGC meta-analysis. First, within the risk locus on chromosome 1q23, two SNPs had substantially stronger signals than others, i.e. rs2274910 ( $P_{NIDDK} = 4.40 \times 10^{-4}$ ) and rs955371 ( $P_{NIDDK} = 4.84 \times 10^{-4}$ ). According to the p-values, these two SNPs are undistinguishable, because the signal at rs2274910 is only slightly stronger. However, the results from the meta-analysis clearly show the existence of two SNP clusters with strong signals at this locus (**Figure 3a**). The cluster closer to gene CD244, in which rs955371 resides, actually has stronger signals than the cluster where rs2274910 is located. Interestingly, the posterior scores capture this difference between two SNPs very well. In fact, the posterior scores for rs955371 and rs2274910 are 0.272 and 0.208, suggesting rs955371 is more likely to be functional even though its p-value is larger. The second example is the risk locus on chromosome 14q35, which is one of the 12 loci with a reduced rank under the posterior scores (**Supplementary Table 2**). Signals at this locus were not strong in the NIDDK study, with the smallest p-value only at  $4.70 \times 10^{-3}$  (rs1959715). Moreover, the signal peak in the NIDDK study (near 88.2M) was quite far from that in the meta-analysis, which resides in genes GALC and GPR65 (**Figure 3b**). However, the posterior scores once again capture the signal pattern in the meta-analysis. Signals near 88.2M on chromosome 14 are shrunk substantially, while the SNPs in GALC and GPR65 are pushed up as the strongest signal (rs4904410). Since these SNPs have very weak signals in their p-values,

the posterior score is still low (See **Methods**). This explains the reduced rank, because the p-value-based rank of rs1959715 was compared with the posterior-based rank of rs4904410. It is worth noting that the SNPs with the strongest signals in the meta-analysis, e.g. rs8005161, were either not genotyped or dropped in the quality control steps in the NIDDK study. It is reasonable to believe that the posterior scores would have had an even better performance if imputations had been done for the NIDDK dataset.

### **Application to schizophrenia**

In addition to Crohn's disease, we also applied GenoWAP to schizophrenia, a major psychiatric disorder. Psychiatric Genomics Consortium (PGC), the largest international consortium in psychiatry, focuses on genetic studies of many psychiatric disorders including schizophrenia. Two large-scale GWAS mega-analyses of schizophrenia have been published. We applied GenoWAP to the earlier and smaller PGC2011 study (Consortium, 2011), and evaluated the performance using results from the larger mega-analyses published in 2014 (Consortium, 2014). Test statistics for both studies were downloaded from the PGC website (**Supplementary Table 3**). Among the 1,252,901 SNPs in PGC2011 study, 264 were removed due to unavailable hg19 locations. Posterior scores were calculated for all the remaining 1,252,637 SNPs (**Supplementary Figure 2**). PGC2014 study contains 9,444,230 SNPs, including 1,179,913 SNPs overlapping with the PGC2011 dataset.

PGC2014 study identified 108 schizophrenia-associated loci, from which we removed three loci on chromosome X because the PGC2011 dataset did not contain any SNP on sex chromosomes. We ranked the 1,252,637 SNPs in PGC2011 study based on their p-values and posterior scores, respectively. Within each locus, the rank of the lowest p-value was compared to the rank of the largest posterior score. Across the 105 loci, 68 (65%) had an improved rank, 1 locus (1%) had an equal rank, and the other 36 loci (34%) had a reduced rank (**Supplementary Table 4**). The probability of having an increased rank is significantly higher than that of having a reduced rank (p-value = 0.001, one-sided binomial test). Interestingly, among the 10 loci with the strongest signals in the PGC2014 study, 8 had an increased rank (80%). The proportion of increased or equal ranks gradually drops when more top loci in the PGC2014 study were considered, showing less confidence in weaker signals (**Supplementary Figure 3**).

Next, we compared the top 20 loci with the smallest p-values to the top 20 loci with the largest posterior scores in the PGC2011 study. In order to identify 20 independent loci, 582 SNPs were needed when using p-value as the criterion. When posterior scores were used to choose top signals, 548 SNPs were sufficient to identify 20 loci, showing better efficiency (**Figure 4a**). A total of 14 loci could be identified using both p-values and posterior scores. As for the comparisons between the 6 posterior-specific loci and the 6 p-value-specific loci, the posterior-specific loci showed better signals than the p-value-specific loci (**Table2, Figure 4b**) in the PGC2014 study. Four of the 6 posterior-specific loci were genome-wide significant in the PGC2014 study, whereas 2 p-value-specific loci passed the genome-wide significance level. Among the 6 p-value-specific loci, the locus

on chromosome 3q26 had the strongest signal in the PGC2014 study ( $P_{2014} = 5.35 \times 10^{-11}$ ). This locus will be discussed in detail later.

Since imputation was done for both PGC2011 and PGC2014 studies, and the total number of SNPs is large, it is possible to compare the SNP-level replication rates when the SNPs were ranked based on p-values and posterior scores. Among the top 500 SNPs with the largest posterior scores, 327, 267, and 152 had a p-value lower than  $5 \times 10^{-2}$ ,  $5 \times 10^{-8}$ , and  $5 \times 10^{-15}$  in the PGC2014 study, respectively. When choosing the top 500 SNPs based on their p-values, the corresponding numbers were 290, 237, and 120 (**Figure 4c**), respectively. A similar pattern can be observed for the top 200 SNPs (**Supplementary Table 4**). We further performed enrichment analysis for whole-blood eQTLs. The top 1000 SNPs based on the p-values were significantly enriched for eQTLs (p-value =  $2.30 \times 10^{-22}$ , fold enrichment = 4.57), but the enrichment for the top 1000 SNPs based on the posterior scores was even stronger (p-value =  $3.32 \times 10^{-25}$ , fold enrichment = 4.88). As the number of top SNPs increased, the posterior-based top SNPs always had stronger enrichment of eQTL than the p-value-based list (**Figures 4d and 4e**).

Finally, we compared PGC2011 p-values, PGC2011 posterior scores, and PGC2014 p-values at two loci to further illustrate the performance of our method. The first locus is on chromosome 3q26. It had the strongest signal in PGC2014 among the p-value-specific top 20 loci (**Table 2**,  $P_{2014} = 5.35 \times 10^{-11}$ ). Based on the p-values in the PGC2011 study, the strongest signals reside in the intergenic region upstream of FXR1. But the posterior scores brought down those intergenic SNPs, and enhanced the signals in FXR1

instead, which is in agreement with the results from PGC2014 (**Figure 5a**). In fact, from the PGC2014 p-values, we can clearly see that the strongest signals reside in FXR1 while the significant results for the SNPs upstream or downstream of FXR1 are likely due to LD. The second example is on chromosome 8q21 (**Figure 5b**). In the PGC2011 study, the strongest signal at this locus resides in the intergenic region between 89.7M and 89.8M. However, posterior scores removed most of the correlated SNPs at this locus, leaving three separate peaks as candidate functional spots. The first peak lies right upstream of MMP16. The second peak is more upstream (~89.6M), and is suggested to be the strongest signal source. The SNPs with the lowest p-values in PGC2011 remained as a signal peak, but their posterior scores were not as strong as the peak in the middle. Most interestingly, the results from the posterior scores perfectly matched the signal patterns in the PGC2014 study. From the lowest panel in **Figure 5b**, we can clearly see two separate peaks at the same locations suggested by the posterior scores, with the one near 89.6M being the strongest signal source. Also, the SNPs between 89.7M and 89.8M had weaker signals than the peak in the middle. Notably, this entire risk locus resides in an intergenic region. This example shows that our method can effectively prioritize SNPs in the non-coding genome.

## Discussion

In this study, we developed and applied GenoWAP to two sets of GWAS data to illustrate its performance in post-GWAS prioritization. Compared to p-values, GenoWAP posterior scores can better prioritize SNPs in many different ways. At the locus level, posterior

score is more efficient in the sense that fewer SNPs are needed to identify the same number of top loci. Moreover, noises due to chance are effectively reduced, and the highly ranked loci using posterior score are more likely to be functional than the top loci selected purely based on p-values. At the SNP level, markers with high posterior scores have both better replication rates and consistently stronger enrichment of eQTLs than the top SNPs based on p-values. More importantly, within each risk locus identified in GWAS, posterior scores can effectively suggest real signals among a large number of correlated SNPs.

The performance of GenoWAP depends on the accuracy of functional annotation and the quality of GWAS data. Due to our limited understanding of non-coding genome, it is challenging to provide accurate genomic functional annotation. GenoCanyon is the first functional prediction tool at the nucleotide level. When more accurate or tissue-specific functional annotation becomes available in the future, the performance of GenoWAP may be further improved. On the other hand, GenoWAP does not play magic. If no information is contained in the GWAS dataset, then GenoWAP can only provide very limited insight.

More than 2,000 GWASs have been published in the past decade, and the number continues to grow. It is well known that our ability to identify new risk loci for complex diseases has surpassed our ability to interpret the results. However, although we are overwhelmed by the large amount of information detected in GWASs, evidence such as missing heritability still suggests that many risk loci remain to be discovered. Therefore,

there is pressing need for post-GWAS prioritization tools and our method has great potential for future application. Since GenoWAP uses only p-values as the input, it is convenient to apply our method on published results, which may help reveal truly functional variants within large haplotype blocks, and ultimately help understand disease etiology. Moreover, for multi-stage GWASs, GenoWAP can be used to better prioritize SNPs from the discovery stage to the validation planning and increase the replication rates. Finally, next-generation sequencing is widely recognized as the future of genomic epidemiology. However, the high cost of sequencing usually leads to insufficient sample sizes and many other challenging issues (Sboner, et al., 2011). The combination of GenoWAP and the rich collection of publicly available GWAS data have the potential to provide functional candidates and guide sequencing analysis in the future.

## **Competing interests**

The authors declare that they have no competing interests.

## **Authors' contributions**

QL conceived and wrote the original manuscript. XY, QL, and YH developed the GenoWAP software. HZ advised on genetic and statistical issues.

## **Acknowledgements**

We would like to thank Dr. Katerina Kechris and all the members in the Data Integration – COPD working group at SAMSI for their advice and useful discussions on this work.

This study was supported by the National Institutes of Health grants R01 GM59507 and U01 HG005718, the VA Cooperative Studies Program of the Department of Veterans Affairs, Office of Research and Development, and the Yale World Scholars Program sponsored by the China Scholarship Council.

## References

- Chung, D., *et al.* GPA: A Statistical Approach to Prioritizing GWAS Results by Integrating Pleiotropy and Annotation. *PLoS genetics* 2014;10(11):e1004787.
- Consortium, S.P.G.-W.A.S. Genome-wide association study identifies five new schizophrenia loci. *Nature genetics* 2011;43(10):969-976.
- Consortium, S.W.G.o.t.P.G. Biological insights from 108 schizophrenia-associated genetic loci. *Nature* 2014;511(7510):421-427.
- Cooper, G.M. and Shendure, J. Needles in stacks of needles: finding disease-causal variants in a wealth of genomic data. *Nature reviews. Genetics* 2011;12(9):628-640.
- Eichler, E.E., *et al.* Missing heritability and strategies for finding the underlying causes of complex disease. *Nature reviews. Genetics* 2010;11(6):446-450.
- Franke, A., *et al.* Genome-wide meta-analysis increases to 71 the number of confirmed Crohn's disease susceptibility loci. *Nature genetics* 2010;42(12):1118-1125.
- Fu, Y., *et al.* FunSeq2: A framework for prioritizing noncoding regulatory variants in cancer. *Genome biology* 2014;15(10):480.
- Hindorff, L.A., *et al.* Potential etiologic and functional implications of genome-wide association loci for human diseases and traits. *Proceedings of the National Academy of Sciences of the United States of America* 2009;106(23):9362-9367.
- Hou, L. and Zhao, H. A review of post-GWAS prioritization approaches. *Frontiers in genetics* 2013;4.
- Kircher, M., *et al.* A general framework for estimating the relative pathogenicity of human genetic variants. *Nature genetics* 2014;46(3):310-315.
- Lu, Q., *et al.* A Statistical Framework to Predict Functional Non-Coding Regions in the Human Genome Through Integrated Analysis of Annotation Data. *Scientific Reports* 2015;5, 10576.
- Manolio, T.A., *et al.* Finding the missing heritability of complex diseases. *Nature* 2009;461(7265):747-753.
- Pruim, R.J., *et al.* LocusZoom: regional visualization of genome-wide association scan results. *Bioinformatics* 2010;26(18):2336-2337.



- Rioux, J.D., *et al.* Genome-wide association study identifies new susceptibility loci for Crohn disease and implicates autophagy in disease pathogenesis. *Nature genetics* 2007;39(5):596-604.
- Ritchie, G.R., *et al.* Functional annotation of noncoding sequence variants. *Nature methods* 2014;11(3):294-296.
- Sboner, A., *et al.* The real cost of sequencing: higher than you think! *Genome biology* 2011;12(8):125.
- Shihab, H.A., *et al.* An Integrative Approach to Predicting the Functional Effects of Non-Coding and Coding Sequence Variation. *Bioinformatics* 2015.
- Visscher, P.M., *et al.* Five years of GWAS discovery. *American journal of human genetics* 2012;90(1):7-24.
- Wang, Q., Lu, Q. and Zhao, H. A Review of Study Designs and Statistical Methods for Genomic Epidemiology Studies using Next Generation Sequencing. *Frontiers in Genetics* 2015;6.
- Ward, L.D. and Kellis, M. Interpreting noncoding genetic variation in complex traits and human disease. *Nature biotechnology* 2012;30(11):1095-1106.
- Witte, J.S., Visscher, P.M. and Wray, N.R. The contribution of genetic variants to disease depends on the ruler. *Nature Reviews Genetics* 2014;15(11):765-776.

## Figures and Tables

**Figure 1. P-value densities of different subgroups of SNPs.** A) P-value histogram of non-functional SNPs ( $Z=0$ , green), p-value histogram of functional SNPs ( $Z=1$ , red), and estimated p-value density of disease-specific functional SNPs ( $Z_D=1$ , blue) in the NIDDK GWAS of Crohn's disease. B) P-value histogram of non-functional SNPs ( $Z=0$ , green), p-value histogram of functional SNPs ( $Z=1$ , red), and estimated p-value density of disease-specific functional SNPs ( $Z_D=1$ , blue) in the PGC2011 GWAS of schizophrenia.

**Figure 2. Global performance in studies of Crohn's disease.** A) Signals at p-value-specific, overlapped, and posterior-specific loci in the IIBDGC meta-analysis. The top 20 loci based on p-values in the NIDDK study are compared with the top 20 loci based on their posterior scores. Each locus is evaluated using the signal strength in the IIBDGC meta-analysis. Darker color indicates stronger signals in the meta-analysis. B) Enrichment of whole-blood eQTLs in the top SNPs selected based on p-value and posterior score. The vertical axis shows the transformed p-value of hypergeometric test. C) Fold enrichment of whole-blood eQTLs in the top SNPs selected based on p-value and posterior score. The vertical axis shows the ratio of observed and expected overlaps between eQTLs and highly ranked SNPs.

**Figure 3. Local performance in studies of Crohn’s disease.** From top to bottom, the three panels show the p-values from the NIDDK study, the posterior scores, and the p-values from the IIBDGC meta-analysis, respectively. A) Local performance at the risk locus on chromosome 1q23. The top two SNPs at this locus in the NIDDK study are undistinguishable based on their p-values. The posterior scores suggest the importance of the SNP on the left, which is in agreement with the results from the meta-analysis. B) Local performance at the risk locus on chromosome 14q35. Signals at this locus are weak in the NIDDK study, and the signal peak is different from that in the meta-analysis. The posterior score is able to pull down the noises caused by LD, and push up real signals at genes GALC and GPR65. Figures are generated using LocusZoom (Pruim, et al., 2010).

**Figure 4. Global performance in studies of schizophrenia.** A) SNPs needed for identifying 20 loci. 582 top SNPs are needed when using p-value as the criterion. 548 SNPs are sufficient when using posterior score as the criterion. B) Signals at p-value-specific, overlapped, and posterior-specific loci in the PGC2014 study. The top 20 loci based on p-values in the PGC2011 study are compared with the top 20 loci based on their posterior scores. Each locus is evaluated using the signal strength in the PGC2014 study. Darker color indicates stronger signals in the large study. C) Replication rates of SNPs before and after prioritization. The top 500 SNPs under posterior scores have substantially higher replication rates than the top 500 SNPs under p-values. D) Enrichment of whole-blood eQTLs in the top SNPs selected based on p-value and posterior score. The vertical axis shows the transformed p-value of hypergeometric test. E) Fold enrichment of whole-blood eQTLs in the top SNPs selected based on p-value and posterior score. The vertical axis shows the ratio of observed and expected overlaps between eQTLs and highly ranked SNPs.

**Figure 5. Local performance in studies of schizophrenia.** From top to bottom, the three panels show the p-values from the PGC2011 study, the posterior scores, and the p-values from the PGC2014 study, respectively. A) Local performance at the risk locus on chromosome 3q26. The top signals at this locus in the PGC2011 study reside upstream of gene FXR1, while the posterior scores pull down those signals and suggest the importance of SNPs in FXR1. This agrees with the signal pattern in the PGC2014 study. B) Local performance at the risk locus on chromosome 8q21. Posterior scores diminish most of the correlated SNPs at this locus, leaving three separate signal peaks. The peak near 89.6M is suggested to be the strongest signal source, which cannot be seen using p-values from the PGC2011 study. The signal peaks suggested by posterior scores perfectly match the strongest signals in the PGC2014 study. Figures are generated using LocusZoom (Pruim, et al., 2010).

**Table 1. The top loci with the strongest signals in the NIDDK study.**

Top 20 loci based on p-value <sup>a</sup>				Top 20 loci based on posterior score <sup>b</sup>			
Chr.	Leading SNP	P <sub>NIDDK</sub>	P <sub>meta</sub>	Chr.	Leading SNP	Posterior	P <sub>meta</sub>
16q12	rs2076756	1.26E-14	4.00E-69	16q12	rs2076756	0.999996866	4.00E-69
1p31	rs7517847	2.99E-13	9.90E-65	1p31	rs7517847	0.999972913	9.90E-65
2q37	rs2241880	4.40E-08	6.70E-41	2q37	rs2241880	0.987698022	6.70E-41
4p13	rs16853571	5.59E-07	2.60E-03	4p13	rs16853571	0.936895112	2.60E-03
12p13	rs886898	1.05E-06	NA <sup>c</sup>	18q21	rs937815	0.911676708	1.40E-05
18q21	rs937815	1.88E-06	1.40E-05	12p13	rs886898	0.890272531	NA <sup>c</sup>
<b>1q23</b>	<b>rs2343331</b>	<b>2.46E-06</b>	<b>1.70E-03</b>	3q23	rs6439924	0.882792742	8.30E-04
3q23	rs6439924	2.89E-06	8.30E-04	1p31	rs2819130	0.773882741	2.20E-03
<b>9q22</b>	<b>rs10821091</b>	<b>9.39E-06</b>	<b>5.40E-04</b>	22q12	rs4821544	0.752640451	1.80E-05
1p31	rs2819130	1.23E-05	2.20E-03	11q13	rs2712800	0.741211726	8.10E-05
<b>14q22</b>	<b>rs1188157</b>	<b>1.23E-05</b>	<b>7.20E-04</b>	<b>9q21</b>	<b>rs4878061</b>	<b>0.697750241</b>	<b>5.20E-04</b>
10q21	rs224136	1.23E-05	4.40E-22	10q21	rs224136	0.663868799	4.40E-22
<b>1q23</b>	<b>rs723821</b>	<b>1.42E-05</b>	<b>1.10E-04</b>	<b>8q22</b>	<b>rs10505007</b>	<b>0.649891635</b>	<b>2.10E-04</b>
22q12	rs4821544	1.71E-05	1.80E-05	<b>15q25</b>	<b>rs3743195</b>	<b>0.630338138</b>	<b>3.80E-03</b>
11q13	rs2712800	1.72E-05	8.10E-05	20q13	rs4810663	0.626012472	2.40E-03
1q31	rs2490271	1.88E-05	7.50E-03	<b>7q36</b>	<b>rs4721</b>	<b>0.622452751</b>	<b>2.30E-03</b>
8q23	rs2044999	1.89E-05	8.40E-04	<b>10q22</b>	<b>rs1250550</b>	<b>0.599609304</b>	<b>2.00E-10</b>
20q13	rs4810663	1.93E-05	2.40E-03	8q23	rs2044999	0.598983918	8.40E-04
<b>16q24</b>	<b>rs8050910</b>	<b>2.00E-05</b>	<b>2.40E-03</b>	1q31	rs2490271	0.58179581	7.50E-03
<b>2p24</b>	<b>rs6733000</b>	<b>2.01E-05</b>	<b>1.90E-02</b>	<b>5p13</b>	<b>rs4613763</b>	<b>0.577762625</b>	<b>7.00E-36</b>

<sup>a</sup>Top 20 loci with the smallest p-values in the NIDDK study. Loci are ordered according to the p-values. Loci in boldface are those not shared in both lists.

<sup>b</sup>Top 20 loci with the largest posterior scores in the NIDDK study. Loci are ordered according to the posterior scores. Loci in boldface are those not shared in both lists.

<sup>c</sup>The IIBDGC meta-analysis does not contain any SNP at this locus.

**Table 2. The top loci with the strongest signals in the PGC2011 study.**

Top 20 loci based on p-value <sup>a</sup>				Top 20 loci based on posterior score <sup>b</sup>			
Chr.	Leading SNP	P <sub>2011</sub>	P <sub>2014</sub>	Chr.	Leading SNP	Posterior	P <sub>2014</sub>
6p22	rs2021722	4.30E-11	3.86E-32	6p22	rs2021722	0.999990069	3.86E-32
8q21	rs7004633	1.45E-08	1.90E-08	10q24	rs11191580	0.998895413	9.24E-18
10q24	rs11191580	2.23E-08	9.24E-18	18q21	rs17512836	0.998854457	9.09E-13
18q21	rs17512836	2.35E-08	9.09E-13	11q24	rs548181	0.998628374	2.87E-05
11q24	rs548181	2.91E-08	2.87E-05	7p22	rs1107592	0.99673362	6.12E-14
7p22	rs10226475	5.06E-08	6.12E-14	15q15	rs1869901	0.991093414	4.92E-08
<b>8p23</b>	<b>rs10503256</b>	<b>1.96E-07</b>	<b>2.69E-08</b>	1p21	rs1625579	0.98743964	2.79E-17
3p14	rs11130874	2.09E-07	7.68E-05	3p14	rs191558	0.987169485	7.68E-05
15q15	rs1869901	3.49E-07	4.92E-08	14q13	rs10135277	0.986756984	1.52E-07
14q13	rs10135277	5.11E-07	1.52E-07	9p24	rs12352353	0.986087806	3.32E-04
1p21	rs1625579	5.72E-07	2.79E-17	12p13	rs4765905	0.980692241	2.63E-17
9p24	rs12352353	6.57E-07	3.32E-04	6p21	rs9462875	0.966743496	9.61E-07
<b>2q31</b>	<b>rs17180327</b>	<b>6.80E-07</b>	<b>5.95E-06</b>	<b>3p21</b>	<b>rs2239547</b>	<b>0.96441905</b>	<b>3.96E-11</b>
12p13	rs7972947	7.77E-07	2.63E-17	8q21	rs4484741	0.96417159	1.90E-08
<b>10q26</b>	<b>rs1025641</b>	<b>8.28E-07</b>	<b>2.21E-04</b>	<b>2q37</b>	<b>rs2675968</b>	<b>0.958718346</b>	<b>3.15E-12</b>
2q37	rs13025591	1.07E-06	3.84E-05	2q37	rs13025591	0.955105149	3.84E-05
<b>11q22</b>	<b>rs2509843</b>	<b>1.10E-06</b>	<b>1.24E-04</b>	<b>1p36</b>	<b>rs2252865</b>	<b>0.939171332</b>	<b>2.03E-09</b>
<b>3q26</b>	<b>rs1879248</b>	<b>1.27E-06</b>	<b>5.35E-11</b>	<b>1q43</b>	<b>rs10803133</b>	<b>0.937014805</b>	<b>4.40E-09</b>
6p21	rs9462875	1.46E-06	9.61E-07	<b>21q22</b>	<b>rs11702343</b>	<b>0.934578026</b>	<b>8.04E-05</b>
<b>11p15</b>	<b>rs4356203</b>	<b>1.90E-06</b>	<b>8.01E-06</b>	<b>22q12</b>	<b>rs9621795</b>	<b>0.925914726</b>	<b>1.26E-03</b>

<sup>a</sup>Top 20 loci with the smallest p-values in the PGC2011 study. Loci are ordered according to the p-values. Loci in boldface are those not shared in both lists.

<sup>b</sup>Top 20 loci with the largest posterior scores in the PGC2011 study. Loci are ordered according to the posterior scores. Loci in boldface are those not shared in both lists.



**Figure 1**

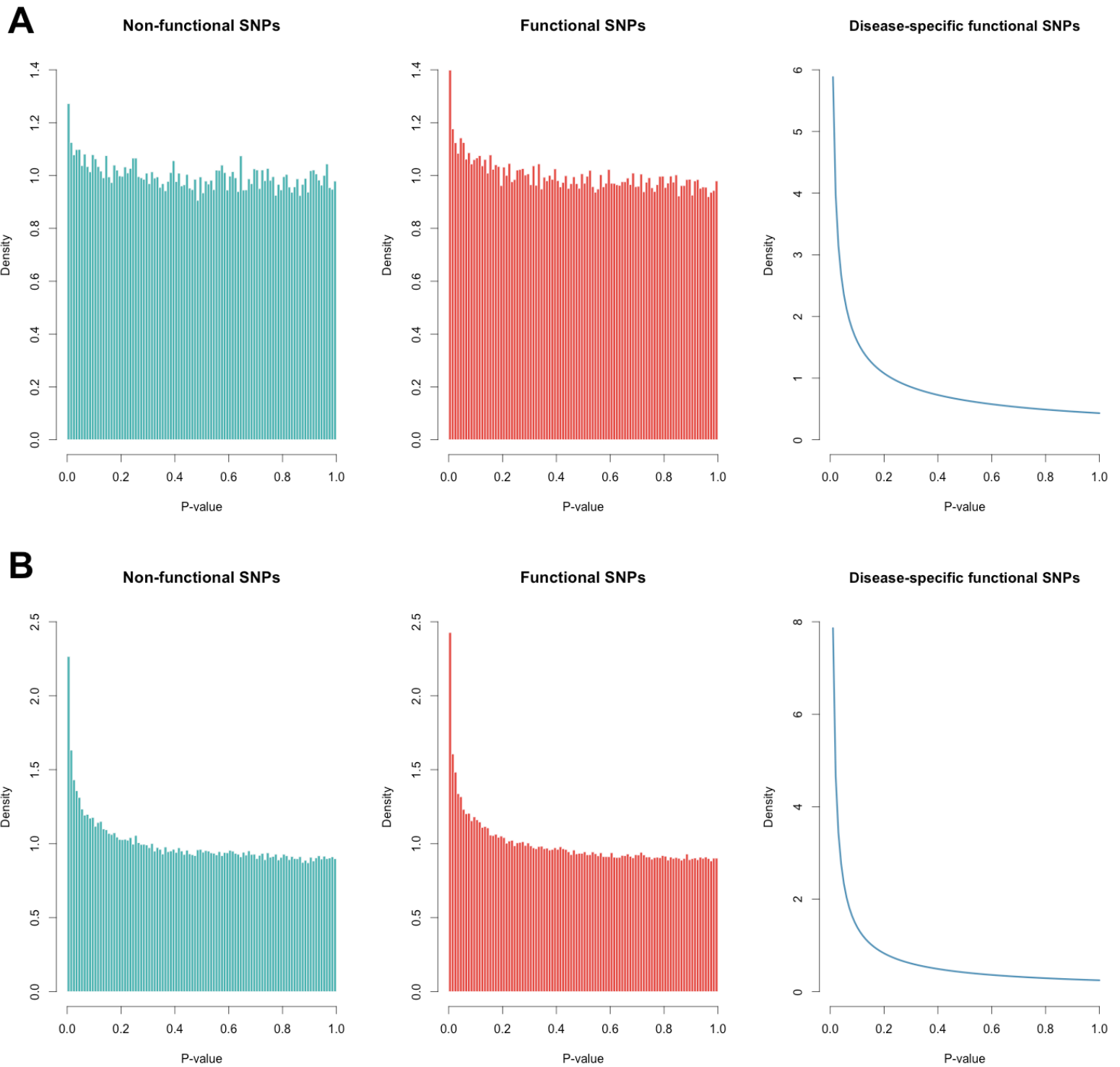


**Figure 2**

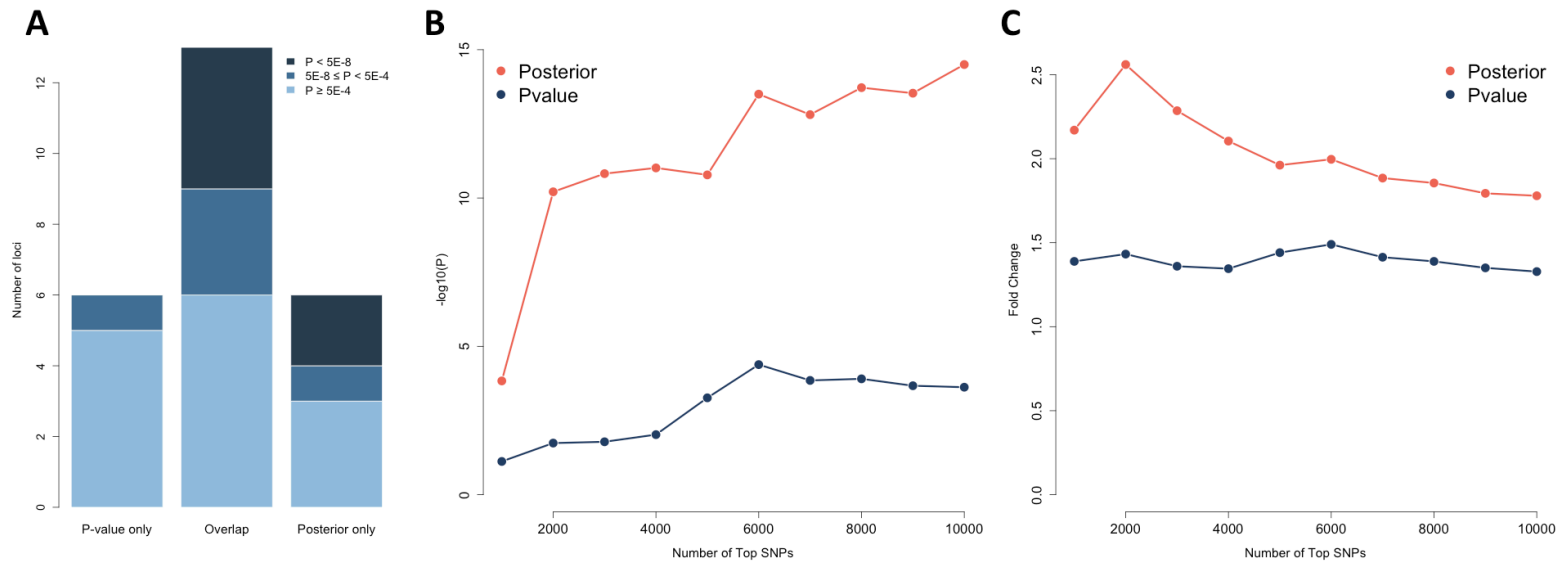
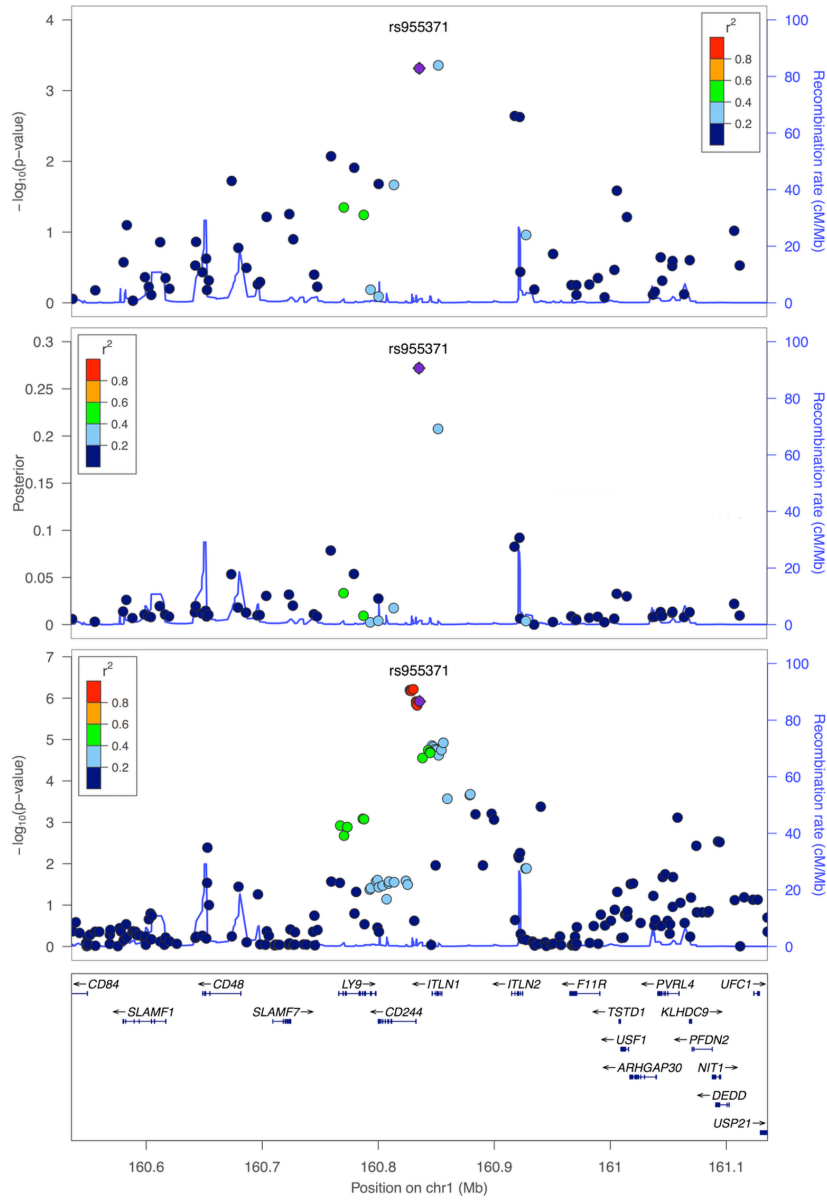


**Figure 3**

**A**



**B**

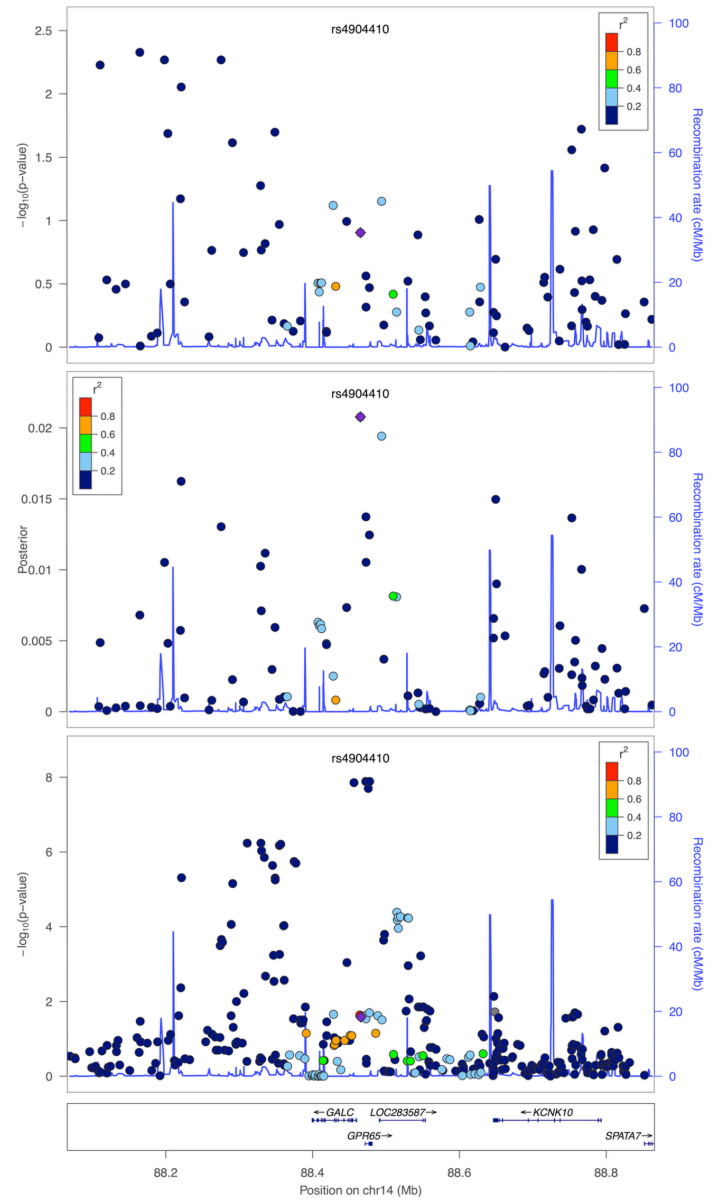


**Figure 4**

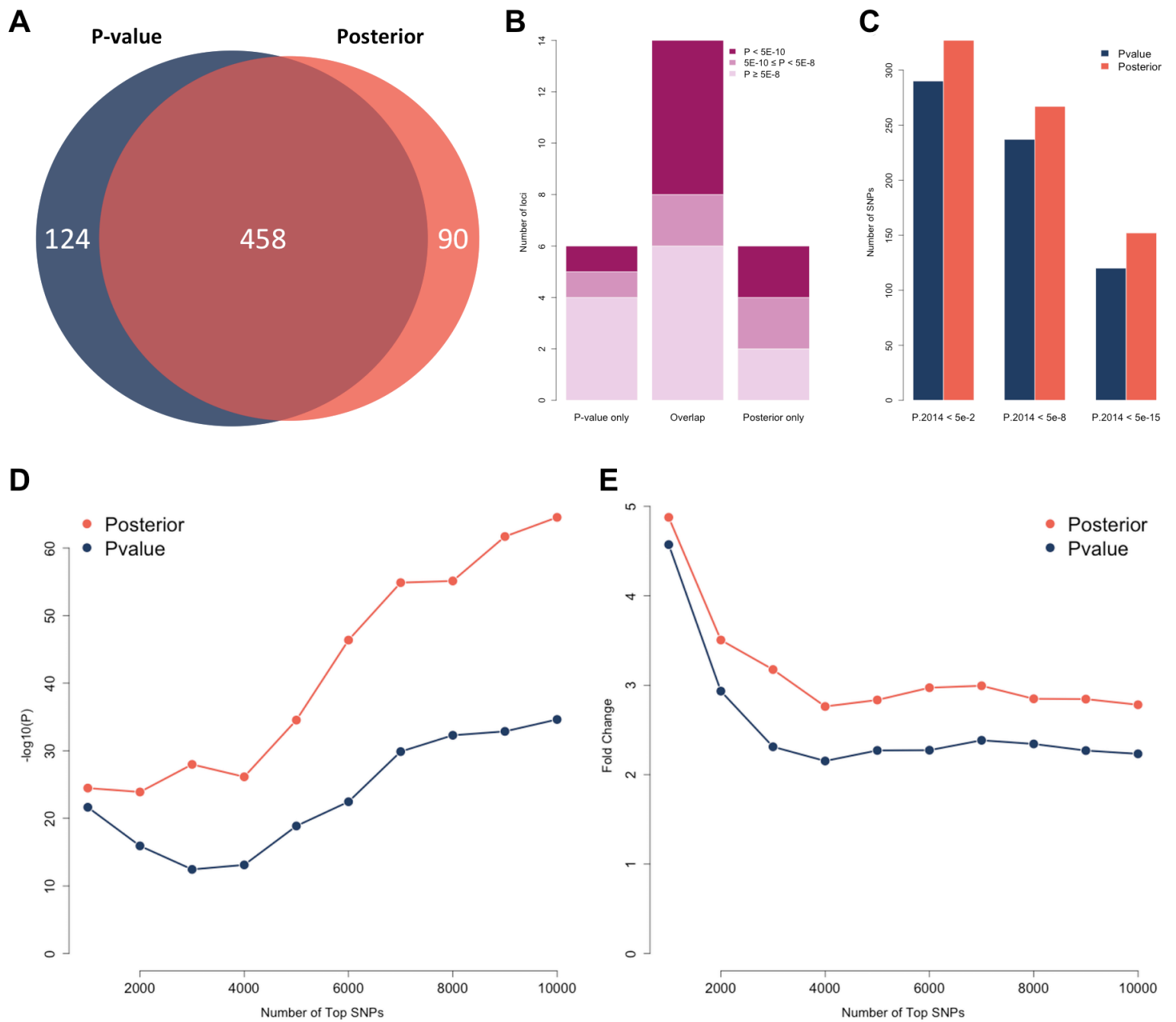
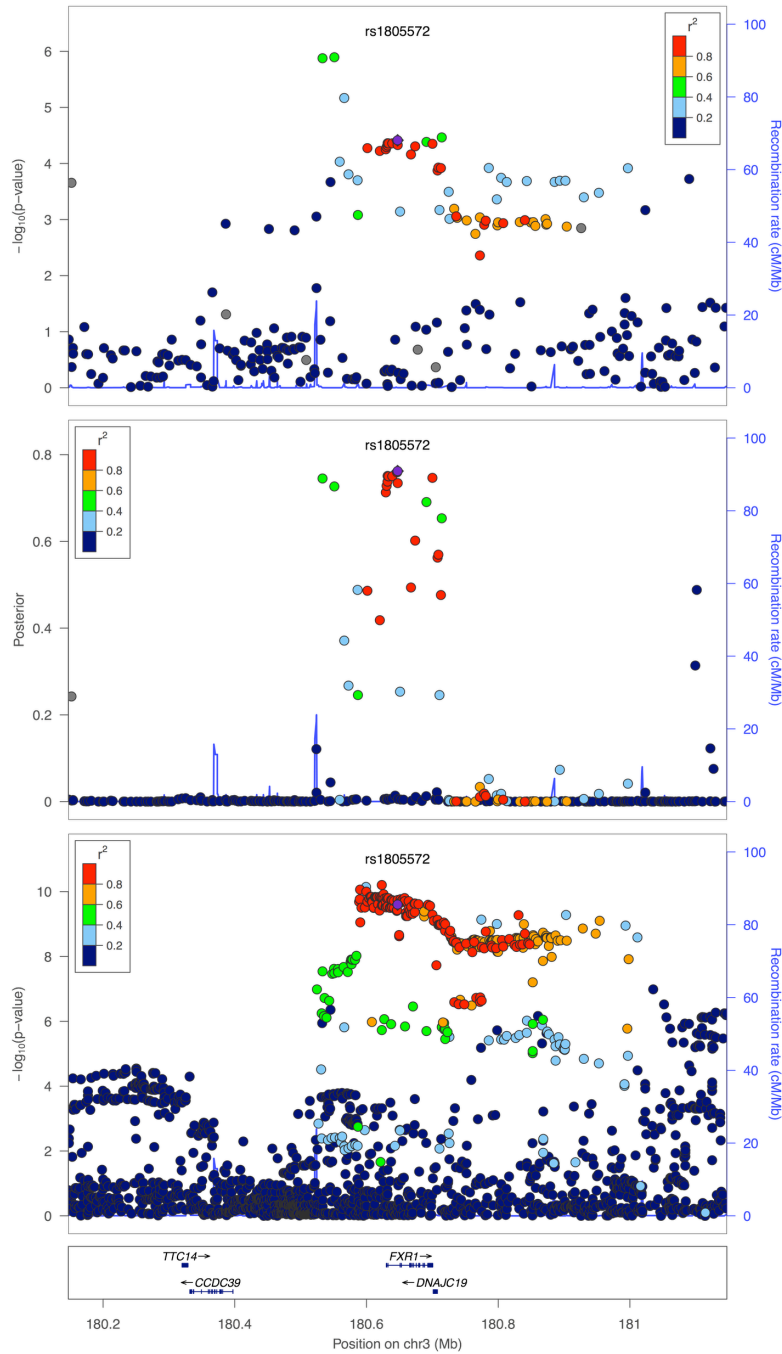
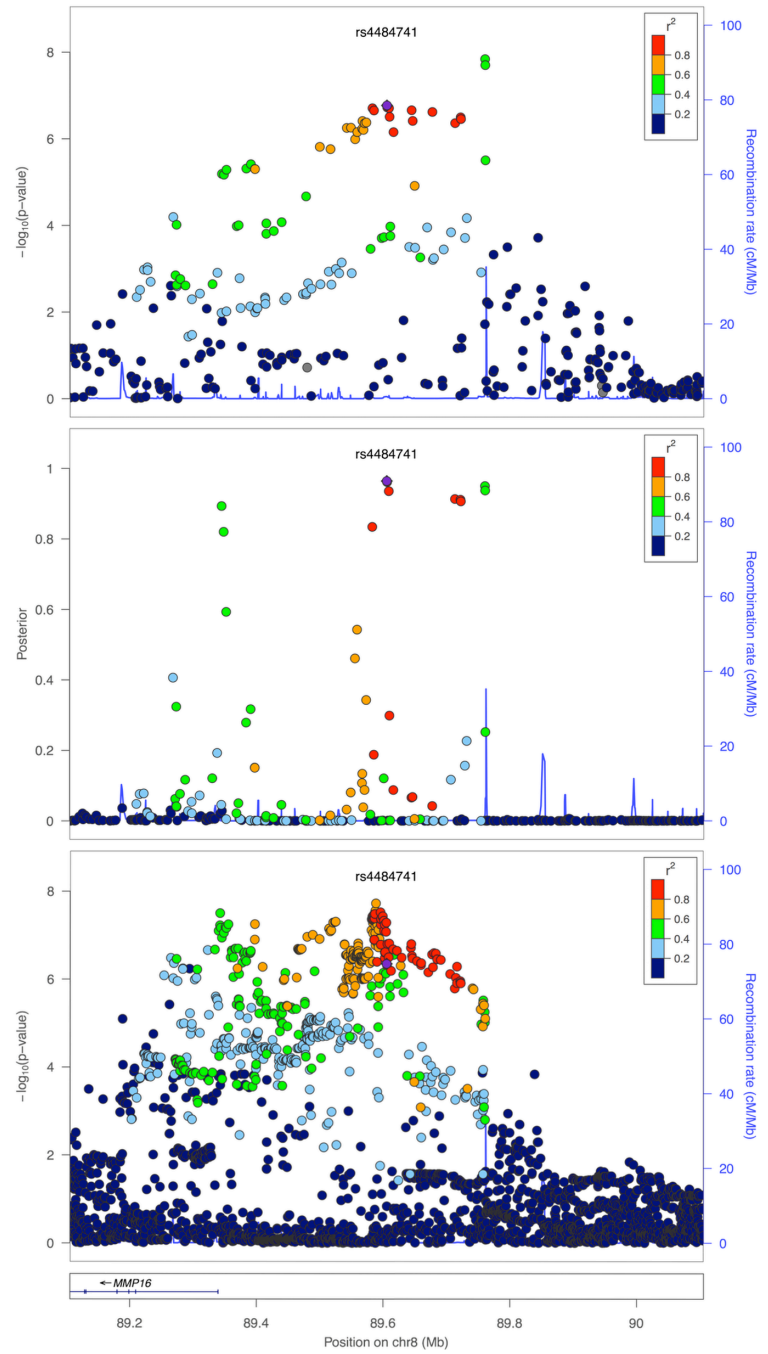


**Figure 5**

**A**

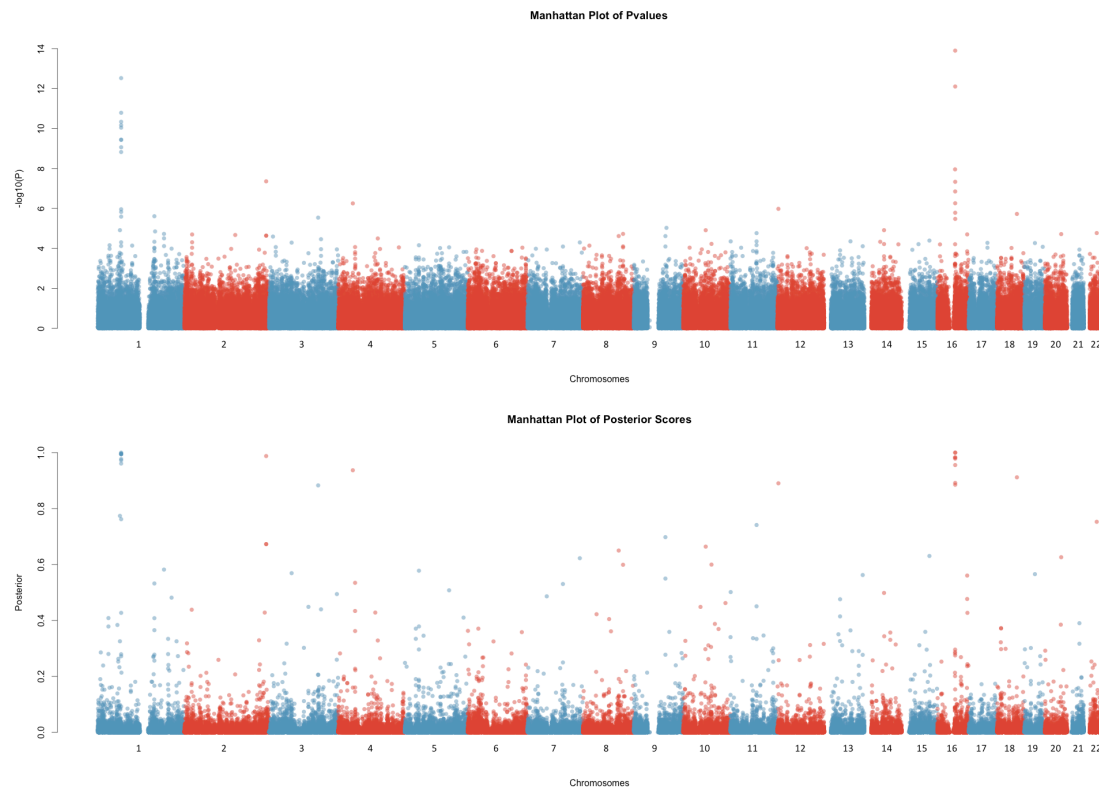


**B**

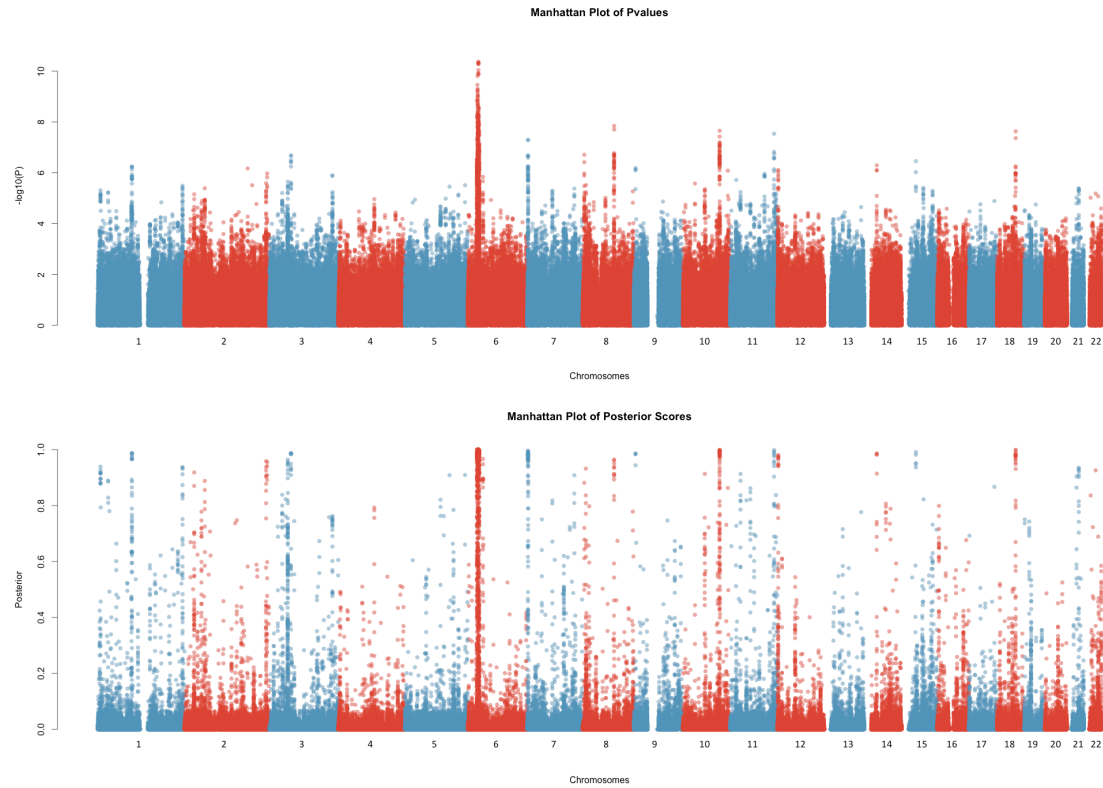


## Supplementary Material

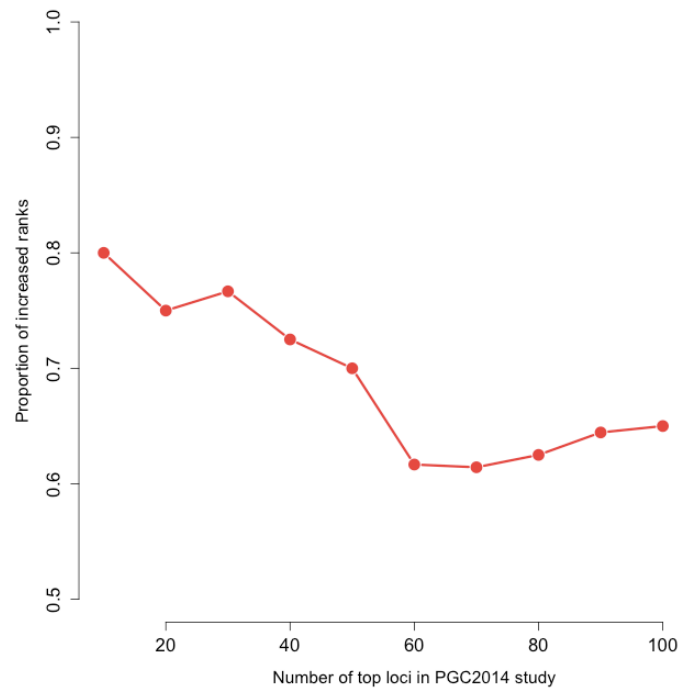
**Supplementary Figure 1.** Manhattan plot of p-values and posterior scores for the NIDDK study.



## Supplementary Figure 2. Manhattan plot of p-values and posterior scores for the PGC2011 study.

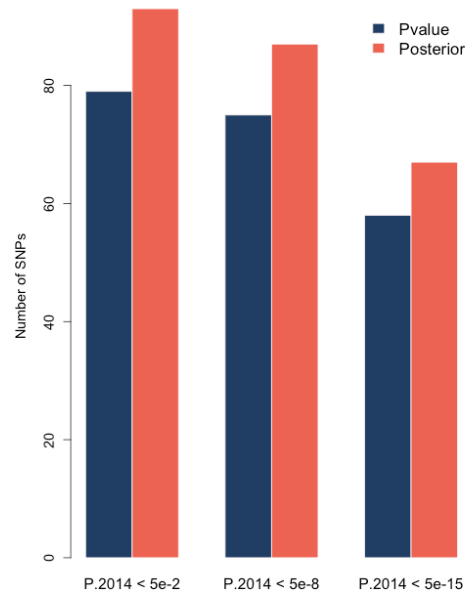


**Supplementary Figure 3.** Negative association between the proportion of increased ranks under posterior score and the number of top loci being considered.





**Supplementary Figure 4.** Enhanced replication rates after prioritization among the top 200 SNPs.



**Supplementary Table 1.** Basic information for NIDDK study and IIBDGC Meta-analysis.

	<b>NIDDK Study<sup>a</sup></b>	<b>IIBDGC Meta-Analysis<sup>b</sup></b>
<b>Disease</b>	Crohn's disease	Crohn's disease
<b># Cases</b>	968 <sup>c</sup>	6,333
<b># Controls</b>	995	15,056
<b>Genotyping Platform</b>	Illumina HumanHap300	Multiple
<b># SNPs</b>	298,391	953,241
<b>Imputation</b>	No imputation	HAPMAP3

<sup>a</sup> The SNP-level summary statistics of the NIDDK study was downloaded from dbGap ([http://www.ncbi.nlm.nih.gov/projects/gap/cgi-bin/study.cgi?study\\_id=phs000130.v1.p1](http://www.ncbi.nlm.nih.gov/projects/gap/cgi-bin/study.cgi?study_id=phs000130.v1.p1)).

<sup>b</sup> The SNP-level summary statistics of the IIBDGC meta-analysis was downloaded from the IIBDGC website (<http://www.ibdgenetics.org>).

<sup>c</sup> The sample size information might be inconsistent with the original publication. The case/control sample size here was extracted from the header lines of the analyses file downloaded from dbGaP.

**Supplementary Table 2.** Ranks of top signals under p-value and posterior score at 71 genome-wide significant loci of Crohn's disease.

Rankings based on p-values				Ranking based on posterior scores		
Chr.	Leading SNP	Pvalue	Rank <sup>a</sup>	Leading SNP	Posterior	Rank <sup>b</sup>
<i>32 previously confirmed Crohn's disease risk loci</i>						
1p31	rs7517847	2.99E-13	2	rs7517847	0.999972913	3
1p13	rs971173	4.44E-03	1954	rs971173	0.114306737	679
1q23	rs2274910	4.40E-04	273	rs955371	0.272006962	154
1q24	rs9286879	8.39E-03	3444	rs9286879	0.072577451	1507
1q32	rs2297909	3.52E-03	1582	rs12122721	0.104187914	796
2q37	rs2241880	4.40E-08	13	rs2241880	0.987698022	9
3p21	rs7629936	4.69E-04	282	rs7629936	0.316858359	111
5p13	rs4613763	6.97E-05	68	rs4613763	0.577762625	38
5q31	rs2243300	8.76E-04	491	rs2243300	0.243962672	184
5q33	rs2112637	1.23E-03	635	rs2112637	0.183061328	283
5q33	rs10045431	1.03E-03	561	rs6556377	0.056512976	2330
6p22	rs6921781	8.76E-03	3578	rs6921781	0.071176737	1554
6p21	rs630379	1.62E-03	781	rs630379	0.186331957	274
6q21	rs2859307	5.53E-03	2373	rs2859307	0.101481811	842
6q27	rs9347189	2.69E-03	1230	rs9347189	0.104526433	788
7p12	rs2045369	1.44E-02	5604	rs10251980	0.035266352	5016
8q24	rs2124036	2.28E-02	8398	rs2124036	0.048432287	2942
9p24	rs2150192	3.47E-03	1557	rs2150192	0.128407135	557
9q32	rs10817694	1.39E-02	5418	rs10817694	0.063059551	1957
10p11	rs2504246	1.01E-03	550	rs2492448	0.040627018	3967
10q21	rs224136	1.23E-05	30	rs224136	0.663868799	30
10q24	rs888208	3.05E-04	201	rs888208	0.369345672	82
11q13	rs1892954	9.91E-04	543	rs6592651	0.130472283	537
12q12	rs545385	6.17E-04	358	rs1444204	0.044793579	3365
13q14	rs583271	1.32E-02	5153	rs3764147	0.048506448	2934
16q12	rs2076756	1.26E-14	1	rs2076756	0.999996866	1
17q21	rs931992	6.32E-03	2687	rs931992	0.094628434	945
17q21	rs9252	4.61E-02	16050	rs9252	0.032894817	5790
18p11	rs9303778	2.88E-03	1305	rs9303778	0.14135767	460
19p13	rs12977033	5.45E-04	324	rs12977033	0.296653851	127
21q21	rs1736148	2.69E-03	1230	rs1736148	0.145846532	435
21q22	rs3827246	1.14E-02	4497	rs3827246	0.07032351	1585
<i>39 Crohn's disease risk loci newly confirmed in the meta-analysis</i>						
1p36	rs707455	4.26E-04	264	rs707455	0.190027644	264
1q22	rs6427128	1.72E-03	833	rs6427128	0.181139121	288
1q31	rs10922341	2.41E-02	8834	rs12568860	0.012105168	36458
1q32	rs4845119	1.07E-02	4287	rs6677934	0.046490815	3156

2p23	rs658414	1.04E-03	564	rs517403	0.12858641	555
2p23	rs780094	3.54E-02	12585	rs2304681	0.026501082	8879
2p21	rs3901678	2.49E-03	1150	rs3901678	0.088740493	1060
2p16	rs13003464	2.32E-03	1085	rs13003464	0.128992257	549
2q12	rs917997	1.55E-03	751	rs13015714	0.124198461	589
2q33	rs700646	3.90E-03	1748	rs770657	0.02803119	8052
2q37	rs16827412	2.69E-02	9748	rs7426302	0.038987848	4243
3p24	rs6792314	8.60E-05	79	rs9881034	0.105980098	773
5q13	rs7702331	1.28E-02	5005	rs638333	0.049480331	2826
5q15	rs4869151	9.50E-03	3857	rs4869151	0.077020627	1358
5q31	rs445310	6.52E-03	2764	rs445310	0.094057648	957
5q35	rs359457	6.94E-04	399	rs359457	0.270517728	156
6p25	rs11242859	4.68E-04	281	rs11242859	0.314623689	114
6q15	rs6939786	5.60E-03	2397	rs6939786	0.099185683	882
6q25	rs7746447	2.39E-03	1110	rs7746447	0.154569531	395
8q24	rs3922389	3.27E-02	11697	rs3922389	0.03981035	4091
9q34	rs4077515	7.33E-04	414	rs4077515	0.264543061	164
10p15	rs4750000	4.27E-04	265	rs4750000	0.326925509	104
10q21	rs11005962	4.46E-03	1960	rs1416764	0.070168232	1591
10q22	rs1250550	5.95E-05	60	rs1250550	0.599609304	35
11q12	rs7947046	1.75E-03	851	rs7947046	0.16782237	338
11q13	rs645078	3.61E-03	1615	rs645078	0.116891493	653
13q14	rs1900448	1.56E-02	6030	rs1900448	0.059300765	2172
14q24	rs174213	3.52E-03	1582	rs174213	0.076308497	1376
14q35	rs1959715	4.70E-03	2057	rs4904410	0.020775196	13706
15q22	rs745103	3.36E-04	219	rs745103	0.359154463	88
16p11	rs151229	2.18E-02	8101	rs151229	0.025564195	9471
17q12	rs991804	3.37E-03	1519	rs991804	0.066547951	1762
19p13	rs6511696	4.76E-03	2077	rs3181049	0.049651701	2809
19q13	rs2287882	4.49E-03	1973	rs17760633	0.089213415	1051
19q13	rs485186	1.95E-03	931	rs504963	0.102902888	816
20q13	rs3810481	1.36E-02	5310	rs3795149	0.062480703	1995
22q11	rs2298428	8.13E-04	462	rs2298428	0.253181625	175
22q12	rs9621049	2.94E-04	196	rs9621049	0.2417048	190
22q13	rs9607601	5.20E-04	307	rs54211	0.151045064	412

<sup>a</sup> rank of the SNP with the smallest p-value

<sup>b</sup> rank of the SNP with the largest posterior score

**Supplementary Table 3.** Basic information for PGC2011 study and PGC2014 study.

	<b>PGC 2011 Study<sup>a</sup></b>	<b>PGC 2014 Study<sup>a</sup></b>
<b>Study Type</b>	GWAS Mega-Analysis	GWAS Mega-Analysis
<b>Disease</b>	Schizophrenia	Schizophrenia
<b># Cases</b>	9,394	34,241 <sup>b</sup>
<b># Controls</b>	12,462	45,604
<b>Genotyping Platform</b>	Multiple	Multiple
<b># SNPs</b>	1,252,901	9,444,230
<b>Imputation</b>	HAPMAP3	1000 Genomes Project

<sup>a</sup> The SNP-level summary statistics of both studies were downloaded from the PGC website (<http://www.med.unc.edu/pgc/>).

<sup>b</sup> These are the number of case-control samples. Besides this, 1,235 parent affected-offspring trios were also included in this study.

**Supplementary Table 4.** Ranks of top signals under p-value and posterior score at 105 genome-wide significant loci of schizophrenia.

Chr.	Start	Stop	Rankings based on p-values			Ranking based on posterior scores			PGC2014 Rank <sup>c</sup>
			Leading SNP	Pvalue	Rank <sup>a</sup>	Leading SNP	Posterior	Rank <sup>b</sup>	
1	2,372,401	2,402,501	rs10910078	2.84E-03	12084	rs10910078	0.105625533	6249	48
1	8,411,184	8,638,984	rs2252865	4.90E-06	714	rs2252865	0.939171332	516	51
1	30,412,551	30,437,271	rs1009080	5.84E-06	746	rs1009080	0.889510826	636	59
1	44,029,384	44,128,084	rs11210896	4.84E-03	17544	rs3001723	0.054816721	12702	44
1	73,766,426	73,991,366	rs11210205	1.25E-03	7070	rs11210274	0.004268122	412743	20
1	97,792,625	98,559,084	rs1625579	5.72E-07	395	rs1625579	0.98743964	242	2
1	149,998,890	150,242,490	rs16835254	1.05E-04	1981	rs7521783	0.587006577	1211	46
1	177,247,821	177,300,821	rs1883243	2.20E-02	53656	rs16851048	0.018150739	59742	98
1	207,912,183	208,024,083	rs2796267	3.81E-04	3724	rs2796267	0.370349774	2010	99
1	243,503,719	244,002,945	rs6703335	3.26E-06	654	rs6703335	0.930827436	534	62
2	57,943,593	58,502,192	rs11682175	4.07E-06	679	rs2683634	0.88791048	640	27
2	72,357,335	72,368,185	rs2241057	2.76E-02	64075	rs2241057	0.032173977	27702	72
2	146,416,922	146,441,832	rs2381759	3.66E-03	14379	rs2381759	0.004539113	377737	56
2	149,390,778	149,520,178	rs12614977	9.92E-03	29507	rs12614977	0.047367587	15941	84
2	162,798,555	162,910,255	rs4664442	7.99E-05	1738	rs2052400	0.507027988	1434	102
2	185,601,420	185,785,420	rs1344706	1.84E-04	2629	rs2369595	0.027291935	34285	17
2	193,848,340	194,028,340	rs17662626	3.09E-06	645	rs17662626	0.007332516	203243	75
2	198,148,577	198,835,577	rs8539	9.97E-04	6166	rs8539	0.22157605	3253	30
2	200,161,422	200,309,252	rs4673339	9.31E-02	166270	rs4673339	0.009291762	146143	74
2	200,715,237	200,848,037	rs11694369	2.15E-03	9958	rs1509835	0.086500653	7519	10
2	225,334,096	225,467,796	rs2047134	1.35E-02	37243	rs16866061	0.04363978	17834	78
2	233,559,301	233,753,501	rs2675968	2.57E-06	621	rs2675968	0.958718346	450	21
3	2,532,786	2,561,686	rs17194476	7.29E-02	136349	rs17620999	0.006866829	221634	33
3	17,221,366	17,888,266	rs17044053	3.88E-03	14986	rs11923589	0.063036738	10203	66
3	36,843,183	36,945,783	rs4624519	6.26E-06	762	rs4624519	0.838545989	698	12
3	52,541,105	52,903,405	rs2239547	2.25E-06	610	rs2239547	0.96441905	427	36
3	63,792,650	64,004,050	rs832197	4.04E-04	3818	rs11922435	0.257087548	2831	82
3	135,807,405	136,615,405	rs10935182	1.23E-04	2154	rs10935186	0.475527492	1548	39
3	180,588,843	181,205,585	rs1351235	8.86E-06	836	rs1805572	0.762139463	816	25
4	23,366,403	23,443,403	rs215451	2.01E-03	9461	rs215478	0.020263667	51863	92
4	103,146,888	103,198,090	rs17823966	9.03E-03	27523	rs170871	0.023889704	41691	6
4	170,357,552	170,646,052	rs3797040	2.68E-04	3116	rs3797040	0.433948011	1694	53
4	176,851,001	176,875,801	rs1106568	4.31E-04	3933	rs2333325	0.064505664	9890	76
5	45,291,475	45,393,775	rs9292918	1.14E-02	32785	rs6451798	0.009397056	143152	70
5	60,499,143	60,843,543	rs34635	8.54E-05	1789	rs7701440	0.544500484	1343	8
5	88,581,331	88,854,331	rs187571	2.90E-02	66539	rs187571	0.028878051	31739	65
5	109,030,036	109,209,066	rs12656073	4.34E-03	16236	rs12656073	0.085565957	7598	91
5	137,598,121	137,948,092	rs13159624	2.38E-03	10684	rs13159624	0.107687062	6135	67
5	140,023,664	140,222,664	rs2337515	4.43E-03	16465	rs17286731	0.080733657	8014	105
5	151,941,104	152,797,656	rs12522297	7.23E-06	791	rs2910032	0.093191565	7022	40
5	153,671,057	153,688,217	rs6863455	4.31E-02	90406	rs6863455	0.018396721	58777	93
6	26,000,000	34,000,000	rs2021722	4.30E-11	1	rs2021722	0.999990069	1	1
6	73,132,701	73,171,901	rs9360557	1.01E-04	1936	rs9360557	0.536308045	1367	89
6	84,279,922	84,407,274	rs217297	7.86E-04	5388	rs2224195	0.028036516	33156	47
6	96,300,000	96,500,000	rs584453	2.35E-03	10575	rs1546898	0.005915849	268799	54
7	1,896,096	2,190,096	rs1107592	5.28E-08	141	rs1107592	0.99673362	125	7
7	24,619,494	24,832,094	rs2721783	5.60E-04	4505	rs2711115	0.223822916	3219	90
7	86,403,226	86,459,326	rs6943762	4.07E-03	15490	rs12704289	0.024224333	40865	42
7	104,598,064	105,063,064	rs4730073	9.81E-05	1900	rs4730073	0.619997851	1105	50
7	110,034,393	110,106,693	rs7783665	1.45E-04	2345	rs7783185	0.080875631	7999	95
7	110,843,815	111,205,915	rs38752	2.82E-04	3202	rs214475	0.414654919	1784	15
7	131,539,263	131,567,263	rs10954343	6.65E-04	4941	rs10954343	0.069858026	9175	97
7	137,039,644	137,085,244	rs320692	2.51E-04	3023	rs320686	0.172770756	4030	60
8	4,177,794	4,192,544	rs10503253	3.84E-07	333	rs10503253	0.516813746	1404	77
8	27,412,627	27,453,627	rs1565735	1.39E-03	7514	rs7844965	0.043300639	18028	88
8	60,475,469	60,954,469	rs7828435	9.82E-04	6114	rs7838646	0.043872025	17687	71

8	89,340,626	89,753,626	rs4484741	1.70E-07	216	rs4484741	0.96417159	428	79
8	111,460,061	111,630,761	rs17392088	3.91E-03	15059	rs13270567	0.003609355	487064	32
8	143,309,503	143,330,533	rs10098073	5.42E-06	736	rs10098073	0.778332214	789	5
9	84,630,941	84,813,641	rs2767713	7.53E-05	1694	rs4877686	0.569316316	1270	61
10	18,681,005	18,770,105	rs7893279	8.08E-04	5469	rs7893279	0.028444957	32514	18
10	104,423,800	104,957,618	rs11191580	2.23E-08	104	rs11191580	0.998895413	69	3
11	24,367,320	24,412,990	rs10834318	1.17E-04	2107	rs10834318	0.231132207	3130	58
11	46,342,943	46,751,213	rs12574668	8.95E-04	5801	rs12574668	0.190473356	3717	24
11	57,386,294	57,682,294	rs11570190	1.66E-05	974	rs11570190	0.861473829	676	57
11	109,285,471	109,610,071	rs1439513	1.69E-03	8492	rs2212430	0.010916963	119181	94
11	113,317,794	113,423,994	rs2514218	8.57E-03	26495	rs4245147	0.025994085	36705	34
11	123,394,636	123,395,986	rs7927176	8.42E-05	1772	rs7927176	0.583233406	1228	73
11	124,610,007	124,620,147	rs11219769	6.39E-02	122871	rs11219769	0.022997524	44197	22
11	130,714,610	130,749,330	rs10791097	2.17E-04	2853	rs10791097	0.472430131	1555	16
11	133,808,069	133,852,969	rs7106715	1.99E-04	2736	rs7106715	0.267248486	2734	35
12	2,321,860	2,523,731	rs4765905	8.92E-07	471	rs4765905	0.980692241	321	4
12	29,905,265	29,940,365	rs436124	1.91E-03	9158	rs302321	0.136143977	5014	96
12	57,428,314	57,682,971	rs324015	3.24E-04	3450	rs324015	0.398537952	1857	19
12	92,243,186	92,258,286	rs4240748	3.81E-03	14776	rs4240748	0.019537175	54405	101
12	103,559,855	103,616,655	rs998499	1.26E-02	35330	rs10860949	0.004407257	394586	104
12	110,723,245	110,723,245	rs4766428	1.93E-03	9249	rs4766428	0.147415196	4640	52
12	123,448,113	123,909,113	rs940904	4.93E-04	4211	rs1727331	0.257456611	2825	9
14	30,189,985	30,190,316	rs2068012	2.54E-02	60026	rs2068012	0.03757315	22470	81
14	72,417,326	72,450,526	rs12896825	2.80E-04	3191	rs4902961	0.10553426	6258	69
14	99,707,919	99,719,219	rs17098461	3.42E-01	490951	rs17098461	0.008175246	176098	68
14	103,996,234	104,184,834	rs4906356	8.41E-04	5586	rs11846404	0.237856661	3040	13
15	40,566,759	40,602,237	rs1869901	3.49E-07	323	rs1869901	0.991093414	194	63
15	61,831,663	61,909,663	rs4775413	4.01E-06	677	rs11071612	0.297931316	2468	43
15	70,573,672	70,628,872	rs1971791	3.27E-02	72789	rs1971791	0.031307514	28593	86
15	78,803,032	78,859,610	rs3813570	6.08E-04	4729	rs3813570	0.285819187	2566	14
15	84,661,161	85,153,461	rs11638630	4.59E-04	4061	rs11631921	0.283185603	2588	28
15	91,416,560	91,429,040	rs8032315	2.84E-03	12100	rs8032315	0.114366082	5836	11
16	9,875,519	9,970,219	rs9938117	6.22E-04	4776	rs11647877	0.237327839	3046	80
16	13,728,459	13,761,359	rs16962588	1.68E-03	8477	rs16962588	0.000392095	892172	49
16	29,924,377	30,144,877	rs12716974	2.20E-03	10117	rs4283241	0.108968991	6075	37
16	58,669,293	58,682,833	rs12447862	3.69E-02	80047	rs12447862	0.010095183	131547	87
16	67,709,340	68,311,340	rs2863981	3.28E-03	13303	rs2863981	0.103787479	6354	83
17	2,095,899	2,220,799	rs11078883	9.46E-04	5987	rs11078883	0.228496217	3159	41
17	17,722,402	18,030,202	rs2955384	5.23E-03	18490	rs2955384	0.057142608	11854	85
18	52,747,686	53,200,117	rs17512836	2.35E-08	106	rs17512836	0.998854457	73	23
18	53,453,389	53,804,154	rs17602354	9.33E-04	5943	rs17602354	0.085071447	7632	29
19	19,374,022	19,658,022	rs2965189	1.57E-04	2439	rs2965189	0.533443545	1373	45
19	30,981,643	31,039,023	rs919803	2.56E-02	60492	rs919803	0.01109558	116888	64
19	50,067,499	50,135,399	rs6509439	1.61E-04	2465	rs11083979	0.355100419	2096	103
20	37,361,494	37,485,994	rs4812319	3.69E-04	3671	rs4812319	0.364286076	2046	26
20	48,114,136	48,131,649	rs576119	1.85E-03	8994	rs576119	0.135692494	5027	100
22	39,975,317	40,016,817	rs5995756	3.67E-04	3661	rs5995756	0.267076671	2735	38
22	41,408,556	41,675,156	rs5758209	8.39E-06	826	rs5758209	0.688851004	971	31
22	42,315,744	42,689,414	rs134902	1.85E-04	2635	rs134902	0.468962552	1568	55

<sup>a</sup> rank of the SNP with the smallest p-value

<sup>b</sup> rank of the SNP with the largest posterior score

<sup>c</sup> rank of 105 loci based on the p-values in the PGC2014 study